Simultaneous micromanipulation in multiple planes using a self-reconstructing light beam

V. Garcés-Chávez, D. McGloin, H. Melville, W. Sibbett & K. Dholakia

School of Physics and Astronomy, University of St Andrews, North Haugh, St Andrews, Fife KY16 9SS, UK

Optical tweezers[1] are commonly used for manipulating microscopic particles, with applications in cell manipulation[2], colloid research[3–5], manipulation of micromachines[6] and studies of the properties of light beams[7]. Such tweezers work by the transfer of momentum from a tightly focused laser to the particle, which refracts and scatters the light and distorts the profile of the beam. The forces produced by this process cause the particle to be trapped near the beam focus. Conventional tweezers use gaussian light beams, which cannot trap particles in multiple locations more than a few micrometres apart in the axial direction, because of beam distortion by the particle and subsequent strong divergence from the focal plane. Bessel beams[8,9], however, do not diverge and, furthermore, if part of the beam is obstructed or distorted the beam reconstructs itself after a characteristic propagation distance[10]. Here we show how this reconstructive property may be utilized within optical tweezers to trap particles in multiple, spatially separated sample cells with a single beam. Owing to the diffractionless nature of the Bessel beam, secondary trapped particles can reside in a second sample cell far removed (~3 mm) from the first cell. Such tweezers could be used for the simultaneous study of identically prepared ensembles of colloids and biological matter, and potentially offer enhanced control of 'lab-on-a-chip' and optically driven microstructures.

Any light beam can be thought of as a superposition of plane waves. As the waves propagate a distance Δz, they undergo a phase shift $k_z\Delta z$, where k_z is the wavevector of the beam in the z direction. In most cases, each plane wave component suffers a different phase shift, and so the resulting beam—the interference pattern of the plane waves—changes shape. There do exist, however, special beams where the phase shift is the same for every plane wave component. These beams do not change shape on propagation, and therefore may be considered diffraction free. For this to happen, the phase shift $k_z\Delta z$ must be the same for all the plane wave components, which can happen if all the waves propagate on a cone. Such a cone can readily be created by illuminating a thin annulus in the front focal plane of a lens. So we can see how such a beam may also be able to reconstruct itself: if part of the beam is blocked, then a shadow is cast into the beam, but the plane waves on the cone that pass the obstruction can reform the beam at a point just beyond the length of the shadow. Such self-reconstruction properties are characteristic of a Bessel beam.

A practical realization of a Bessel beam[11] can be produced by illuminating a conical shaped optical element, called an axicon, with a gaussian beam[12]. The beam produced is a close approximation to a Bessel beam over a characteristic propagation distance. The central maximum propagates for several Rayleigh ranges without appreciable divergence, and thus approximates a rod of light. The outer rings of the Bessel beam act to replenish the central maximum and prevent it from spreading. This replenishment also allows the Bessel beam to reconstruct itself if blocked[13]. If a beam has an object, of radius r_{ob}, placed at its centre, then the object will cast a shadow of length l_s into the beam:

$$l_s \approx \frac{r_{ob}k}{k_r} \quad (1)$$

where k_r is the radial wavevector of the beam, with a wavevector $k = (k_r^2 + k_z^2)^{1/2}$.

After this distance the beam will have reformed, and will continue to propagate without diffraction over its remaining propagation distance. In Fig. 1 we show a numerical simulation of a zeroth-order obstructed Bessel beam. We could also use high-order Bessel beams, which have an intensity minimum on axis—such beams also reconstruct when blocked. In addition, there are other families of diffractionless beams, such as the Mathieu beams[14], which have properties comparable to (but distinct from) Bessel beams and that can be used similarly to the work presented here. We are also able to generate other patterns of diffractionless beams, notably by creating interference patterns (between two other non-diffracting beams of opposite helicity) that have a number of spots equal to twice the azimuthal index of the interfering beams (D.M., V.G.-C. and K.D., manuscript in preparation). By using spatial light modulators[15], it is possible to create arrays of Bessel beams in any desired pattern, adding a greater generality to our technique.

Bessel beams can be used as simple two-dimensional optical tweezers[16]. As they are propagation invariant, they act as a rod of light and have no confining force in the beam propagation direction. We are able to create tweezers in two differing geometries. Standard (downward) tweezers push (via radiation pressure) the samples down against the microscope slide. Inverted (upward) tweezers are used to levitate, align, stack and guide particles, again

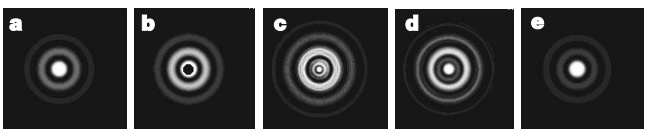

Figure 1 Beam propagation simulation. Numerical simulation of the propagation of a Bessel beam that has its central maximum blocked. **a**, Bessel beam before the obstruction—a set of concentric rings surrounding a bright central spot. **b**, Obstruction placed over the central spot. **c**–**e**, The beam at various positions beyond the obstruction. The beam is seen to distort, and then reform in **e**. Boxes are 0.75 mm squares.

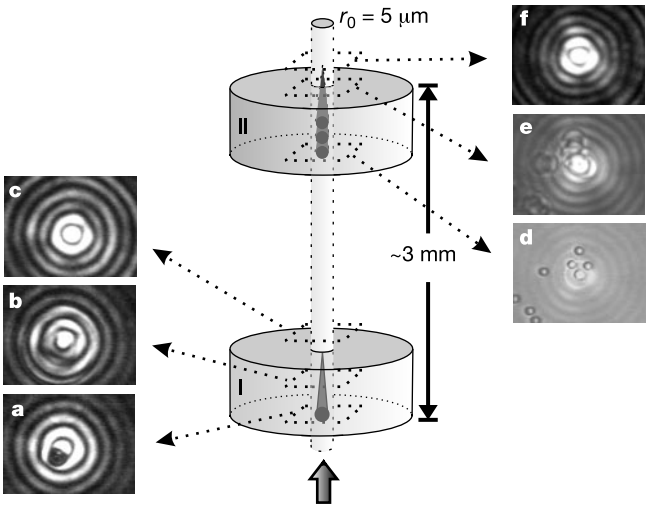

Figure 2 Inverted tweezers experimental set-up. Main figure, set-up for manipulation of particles that have large spatial separations. The cells (I and II) are 3 mm apart, and 100 μm deep. **a**–**f**, Frames from a video taken of objects captured by the Bessel beam; control spot radius $r_0 = 5$ μm. **a**, A hollow sphere ($n < 1$) of ~5 μm diameter is trapped in cell I between the central spot and the first ring of the Bessel beam. Note that n is the relative refractive index between the particle and the suspending medium. **b**, The beam a short distance above **a**. Here the beam has been distorted by the particle. **c**, Some small distance above the first sample cell, the beam has reformed and is no longer distorted. **d**, The beam enters the cell II, and is able to stack three 5-μm-diameter solid silica spheres. **e**, **f**, The beam profile above the stack of particles. The beam has reformed once more.

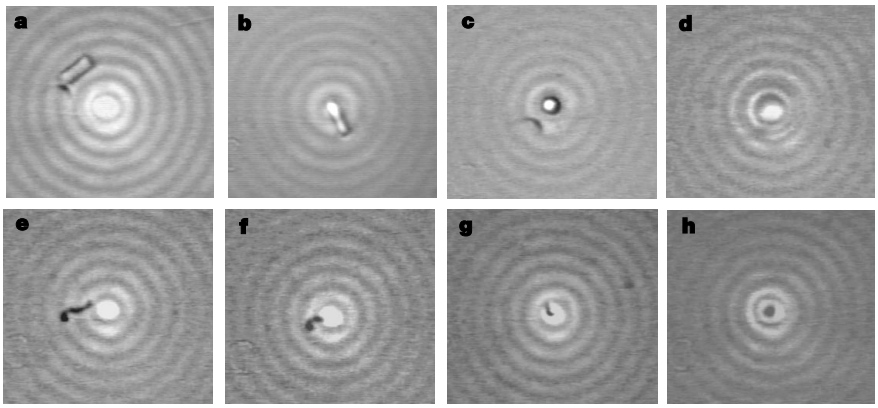

Figure 3 Alignment of glass rods and chromosomes. Sequence of frames taken from a video of optical manipulation in two separated cells (Fig. 2). Frames **a**–**c** and **e**–**h** show particles being attracted to the central spot of the Bessel beam, and then aligning themselves with the beam. The lower cell (top row) contains a glass rod of ~8 μm length; the upper cell (bottom row) contains a Muntjac deer chromosome. **a**, The profile of the beam entering the bottom cell. **b**, the glass rod trapped in the central maximum of the Bessel beam; it is eventually rotationally aligned along the beam direction (**c**). **d**, The distorted beam after passing the confined rod. The beam continues to propagate to the top cell (**e**), where the chromosome is evident. **f**–**h**, The subsequent trapping and rotational alignment of the chromosome.

making use of radiation pressure in the direction of the beam. For the observations reported here we use both geometries, with a basic experimental set-up described previously[16]. An axicon is illuminated with a power of up to 1 W from a 1,064-nm-wavelength laser. Telescoping optics before the axicon allow us to vary the propagation length of the Bessel beam. A variable-magnification telescopic system is placed after the axicon, allowing us to reduce the size of the central maximum. In this manner we can readily adjust the parameters of the Bessel beam that is incident on the sample slide. The maximum power at the sample plane was about 700 mW, which is spread evenly among the rings, with a maximum of about 35 mW found in the central spot of the Bessel beam. The power measured after each reconstruction of the beam is approximately the same. We are able to control the power in the rings by changing the number of rings in the Bessel beam. Decreasing the number of rings will increase the power in each ring (and the central spot), but this comes at the expense of a decrease in propagation distance. A microscope objective and CCD (charge-coupled device) camera are used to observe the trapped particles on a video monitor.

We discuss our experimental results on Bessel beam optical tweezers in both the inverted and the standard geometries. Figure 2 shows results, in the inverted geometry, using two sample cells 3 mm apart. Low-refractive-index (with respect to the suspending medium) particles are in the bottom cell, and 5-μm-diameter silica spheres are in the top cell. Each cell was ~100 μm deep. We used a Bessel beam with a central radius of ~5 μm and a propagation distance of about 4 mm. The beam profile was distorted by the low-refractive-index particle, and reconstructed 100 μm beyond it. Using exactly the same beam and after passing the bottom cell, we have stacked up to three 5-μm spheres above one another, in a one-dimensional array, in the top cell, and manipulated this whole particle chain while still manipulating in unison the low-refractive-index particle trapped in the first cell. We note that the separation distance between the cells (3 mm) is ~40 times the Rayleigh range of a gaussian beam with a 5-μm beam waist.

We also observe the ability to use these tweezers to align rod-shaped particles in multiple cells. Many biological specimens have such forms, and by using Bessel beam tweezers the rods can be aligned along the propagation direction of the beam[16]. This is achieved using a single stationary beam—when trapped, the particles are held simultaneously. (This is in contrast to the single particle that could be aligned with a gaussian beam.) They can then be moved in unison by translation of the sample cells. Here we use a Bessel beam with a propagation distance of ~10 mm, using the same cell set-up (Fig. 2). In the bottom cell, we have fragments of glass rod that are approximately 8 μm in length, and in the top cell we have Muntjac deer chromosomes. Figure 3 shows the alignment of the rods and chromosomes in their respective cells.

Using the downward tweezers geometry, we observed tweezer action in three separate cells—again each ~100 μm in depth, with ~10-μm cover glass slips as separators—stacked one on top of the other. The top cell contains 5-μm-diameter solid silica spheres. In the second cell are 2–20-μm-diameter hollow silica spheres, and in the third cell are birefringent (calcite, ~5 × 4 μm) particles. We are able to trap particles in all three traps simultaneously and manipulate them.

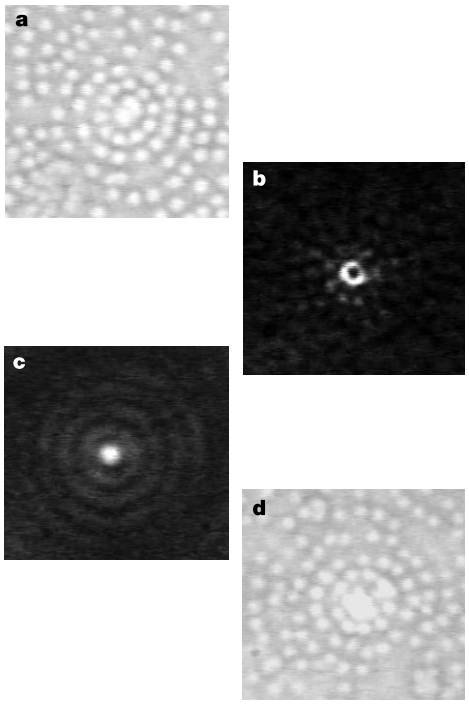

Figure 4 Arrays of 1 μm spheres. **a**–**d**, Successive frames taken from a video, with the trapping beam passing through two cells containing 1-μm spheres in water. The set-up uses the standard, downward geometry, tweezers. The two cells are separated by 100 μm. **a**, The bottom of the upper cell. The beam profile is distorted (**b**), and subsequently self-reconstructs (**c**) below the first cell. **d**, The pattern created in the lower cell. Frames **a** and **d** appear bright as an extra white-light source is used to see the sample. Notice that the beam is able to form a two-dimensional array in each cell.

Our single laser beam can trap particles of varying refractive index, which cannot be done with a single gaussian beam. Hollow spheres (relative refractive index $n < 1$) cannot be trapped by a normal gaussian beam, because regions of high intensity repel such particles. By contrast, we are able to trap such particles with our Bessel beam—between the bright rings, in the dark regions when the sphere diameter exceeds the bright ring spacing. We also note that we are not only able to trap the birefringent particle at the bottom of the third cell, but we can rotate it as well, using a circularly polarized Bessel beam. We thus impart angular momentum to the particle[17]. The different types of particle have specific reconstruction distances, indicating that the reconstruction distance is, at least in part, dependent on the refractive index of the particle. Owing to the differing distortion and shadowing of a Bessel beam by different types of particles, there is the prospect of using the self-reconstructing beam as a means to characterize particles or cells. The number of particles we can trap is limited, but only by the available laser power and the propagation distance of the Bessel beam. The size of the obstruction ultimately represents a limitation, because if the entire beam is blocked then we could not expect any subsequent reconstruction. Particles that we can trap with tweezers are generally at least partially transparent, and hence even if the sample cell is filled with particles the transmitted beam is still able to reconstruct. We show in Fig. 4 a dense sample (~20% of the sample area) of 1-μm-diameter silica spheres that cover the observable Bessel beam in the cell. The particles are trapped in the rings of the Bessel beam, forming a two-dimensional planar array. We then see an image from a sample cell 100 μm below the top cell also filled with 1-μm-diameter silica spheres. We see that these particles can be manipulated, and also that the Bessel beam is able to reform. The power in the reformed Bessel beam is ~90% (630 mW) of the power of the beam incident on the first cell. Thus we have created multiple planes of 2D arrays where the planes of the array are separated by the depth of the sample cell.

As mentioned above, we have the ability to rotate birefringent particles by transference of spin angular momentum from the beam to the particle in a multi-cell system. A more interesting extension of this work is to interfering Bessel beams. Recent work[18,19] has shown that by interfering high-order Laguerre–Gaussian beams it is possible to create interferometeric patterns that consist of arrays of spots. These can be used to rotate particles, which need not be birefringent, in a controlled fashion, or alternatively to create three-dimensional structures. We can also create such patterns with Bessel beams, and have used these to rotate particles (D.M., V.G.-C. and K.D., manuscript in preparation). This opens up the possibility of the controlled rotation of systems (that is, micromachines), or the guidance and alignment of streams of particles, or cold atoms, over extended distances in unison. Using Bessel beams for rotational studies of particles may be of particular practical interest. We are able to rotate particles in multiple cells, rotating many objects simultaneously, thereby opening up the possibility of arrays of micromachines. Such beams could act on more complex microstructures. For example, imagine two micro-cogs, attached by an axle rod. As the Bessel beam reconstructs itself, we could use the same beam to drive both cogs simultaneously and with the same rotation speed.

Self-reconstructing optical tweezers could also be applied to other avenues of research. For example, it may be possible to conduct simultaneous studies of identically prepared samples, in different cells, with each cell having a different ambient condition—such as temperature. We have shown how arrays of particles may be created, which could have applications in colloid physics and in bioengineering. This work could be readily extended to the creation of large three-dimensional arrays. Conventionally this is difficult. Recent work[15,20] has shown that by using holographic beam shaping techniques, two-dimensional planar arrays can be created. These can also be dynamically controlled. An array of such dynamic tweezers, making use of reconstructing Bessel beams, would represent a controllable three-dimensional structure, and could have significant application in, for instance, the control of arrays of lab-on-a-chip microstructures and micromachines. □

Received 10 May; accepted 23 July 2002; doi:10.1038/nature01007.

1. Ashkin, A., Dziedzic, J. M., Bjorkholm, J. E. & Chu, S. Observation of a single-beam gradient force optical trap for dielectric particles. *Opt. Lett.* **11,** 288–290 (1986).
2. Smith, S. B., Cui, Y. & Bustamante, C. Overstretching B-DNA: The elastic response of individual double strained and single stranded DNA molecules. *Science* **271,** 795–799 (1996).
3. Crocker, J. C. & Grier, D. G. Methods of digital video microscopy for collodial studies. *J. Colloid Interf. Sci.* **179,** 298–310 (1996).
4. Crocker, J. C., Matteo, J. A., Dinsmore, A. D. & Yodh, A. G. Entropic attraction and repulsion in binary colloids probed with a line optical tweezer. *Phys. Rev. Lett.* **82,** 4352–4355 (1999).
5. Larsen, A. E. & Grier, D. G. Like charge attractions in metastable colloidal crystallites. *Nature* **385,** 230–233 (1997).
6. Friese, M. E. J., Rubinsztein-Dunlop, H., Gold, J., Hagberg, P. & Hanstorp, D. Optically driven micromachine elements. *Appl. Phys. Lett.* **78,** 547–549 (2001).
7. Volke-Sepulveda, K., Garcés-Chávez, V., Chávez-Cerda, S., Arlt, J. & Dholakia, K. Orbital angular momentum of a high-order Bessel light beam. *J. Opt. B* **4,** 582–589 (2002).
8. Durnin, J., Miceli, J. J. Jr & Eberly, J. H. Diffraction-free beams. *Phys. Rev. Lett.* **58,** 1499–1501 (1987).
9. McQueen, C. A., Arlt, J. & Dholakia, K. An experiment to study a "nondiffracting" light beam. *Am. J. Phys.* **67,** 912–915 (1999).
10. Bouchal, Z., Wagner, J. & Chlup, M. Self-reconstruction of a distorted nondiffracting beam. *Opt. Commun.* **151,** 207–211 (1998).
11. Durnin, J. Exact solutions for nondiffracting beams. I. The scalar theory. *J. Opt. Soc. Am. A* **4,** 651–654 (1987).
12. Herman, R. M. & Wiggins, T. A. Production and uses of diffractionless beams. *J. Opt. Soc. Am. A* **8,** 932–942 (1991).
13. MacDonald, R. P., Boothroyd, S. A., Okamato, T., Chrostowski, J. & Syrett, B. A. Interboard optical data distribution by Bessel beam shadowing. *Opt. Commun.* **122,** 169–177 (1996).
14. Chávez-Cerda, S. *et al.* Holographic generation and orbital angular momentum of high-order Mathieu beams. *J. Opt. B* **4,** S52–S57 (2002).
15. Curtis, J. E., Koss, B. A. & Grier, D. G. Dynamic holographic optical tweezers. *Opt. Commun.* **207,** 169–175 (2002).
16. Arlt, J., Garcés-Chávez, V., Sibbett, W. & Dholakia, K. Optical micro-manipulation using a Bessel light beam. *Opt. Commun.* **197,** 239–245 (2001).
17. Friese, M. E. J., Nieminen, T. A., Heckenberg, N. R. & Rubinsztein-Dunlop, H. Alignment or spinning of laser-trapped microscopic waveplates. *Nature* **394,** 348–350 (1998).
18. Paterson, L. *et al.* Controlled rotation of optically trapped microscopic particles. *Science* **292,** 912–914 (2001).
19. MacDonald, M. P. *et al.* Creation and manipulation of three-dimensional optically trapped structures. *Science* **296,** 1101–1103 (2002).
20. Korda, P., Spalding, G. C., Dufresne, E. R. & Grier, D. G. Nanofabrication with holographic optical tweezers. *Rev. Sci. Instrum.* **73,** 1956–1957 (2002).

Acknowledgements

We thank G. Spalding for discussions. This work was supported by the Leverhulme Trust, the UK Engineering and Physical Sciences Research Council and the Medical Research Council.

Competing interests statement

The authors declare that they have no competing financial interests.

Correspondence and requests for materials should be addressed to K.D. (e-mail: kd1@st-and.ac.uk).

Mechanical milling assisted by electrical discharge

A. Calka & D. Wexler

Faculty of Engineering, University of Wollongong, Wollongong, New South Wales 2522, Australia

Mechanical milling is an effective technique for the preparation of fine metallic and ceramic powders and can also be used to drive a wide range of chemical reactions. Milling devices include planetary machines, attritors and vibrational mills; products include amorphous, nanocrystalline and quasicrystalline materials, supersaturated solid solutions, reduced minerals,